Journal of Physics: Conference Series **3094** (2025) 012019 doi:10.1088/1742-6596/3094/1/012019

Electron beam scattering in Rubidium vapour at AWAKE

N. Z. van Gils[1,2], M. Moreira[2], M. Turner[2], E. Gschwendtner[2], L. Ranc[3], J. Mezger[3], M. Bergamaschi[2,3], P. Muggli[3], D. Cooke[4], F. Pannell[4] and A. Gerbershagen[1]

[1] PARTREC, UMCG, University of Groningen, Groningen, NL
[2] CERN, Geneva, CH
[3] Max Planck Institute for Physics, Munich, DE
[4] University College London, London, UK

E-mail: nikita.zena.van.gils@cern.ch

Abstract. The Advanced Wakefield Experiment (AWAKE) at CERN uses bunches from the CERN SPS to develop proton-driven plasma wakefield acceleration. AWAKE Run 2c (starting in 2029) plans for external on-axis injection of a 150 MeV electron witness bunch with the goal to demonstrate emittance control of multi-GeV accelerated electron beams. Prior to injection, the electron witness bunch may have to traverse rubidium vapour. Since the beam must have the correct beam size and emittance at injection, it is important to quantify the scattering effect. For this, first-principle estimates and GEANT4 simulations are compared with measurements of a ∼20 MeV electron beam scattering in 5.5 m of rubidium vapour, showing good agreement. Building on this agreement, GEANT4 simulations using the estimated AWAKE Run 2c parameters are performed. These predict that scattering will not increase the electron beam size or emittance.

1. The AWAKE experiment and motivation

The Advanced Wakefield Experiment (AWAKE) at CERN aims to develop proton driven plasma based wakefield acceleration. AWAKE successfully conducted proof-of-principle experiments in Run 1 (2016–2018) [1]. Currently, in Run 2 (2021–2033), the focus is to start transitioning to practical accelerator applications [2]. From Run 1 to Run 2b, a single rubidium plasma was used for both proton bunch self-modulation and electron beam acceleration. While electrons were accelerated to several GeV, the required external side-injection scheme [3] caused large emittances [4, 5].

The goal of the next phase, Run 2c (2029–2031), is to demonstrate acceleration of a witness bunch to multi-GeV energies while controlling the emittance. This is possible by injecting the witness beam on axis and matching it to the wakefields, e.g. with a normalised emittance $\varepsilon_N = 2\,\text{mm mrad}$ and a one sigma waist size $\sigma_{x,y} \sim 5\,\mu\text{m}$, as proposed in Ref. [6]. The electron source and beamline have been designed to achieve these values [7].

The injection experiment will involve two 10 m long plasmas, one for proton bunch self-modulation [8, 9, 10] and one for acceleration of the witness bunch. In between the two plasmas, a 150 MeV electron bunch will be brought on the same trajectory as the proton bunch. In the baseline plasma sources design, rubidium vapour would be present between the two plasmas.

This paper explores whether scattering of the electron beam in rubidium vapour would significantly increase the witness beam size and emittance for AWAKE Run 2c. This study matters for Run 2c to ensure witness beam emittance is preserved despite traveling through the vapour. It is subdivided into three sections. First, the mean scattering angle is estimated analytically. Second, measurements of a ∼20 MeV electron beam are performed with the current AWAKE setup and compared to GEANT4 simulations. Third, further GEANT4 simulations are performed for parameters close to the Run 2c setup. Based on these inputs, conclusions for the AWAKE Run 2c design are drawn.

2. First-principle estimate

The radiation length X_r quantifies how much material must be traversed for a high-energy electron to lose most ($1 - 1/e \approx 0.63$) of its energy due to bremsstrahlung. For a pure material with density n, X_r can be estimated with [11, 12]:

$$X_r = \frac{1}{4\alpha r_e^2 n} \left\{ Z^2 \left[L_{\text{rad}} - f(Z) \right] + Z L'_{\text{rad}} \right\}^{-1}, \tag{1}$$

where α is the fine-structure constant, r_e is the classical electron radius, Z is the atomic number of the material, and $f(Z)$, L_{rad} and L'_{rad} are formulas that depend on α and Z (see Sec. 34.4.2 of Ref. [12] for more details).

The radiation length of solid rubidium is $X_{r,\text{solid}} = 7.198\,\text{cm}$. For rubidium vapour with density $n = 1\text{–}10 \times 10^{14}\,\text{cm}^{-3}$ (typical for AWAKE), $X_{r,\text{vapour}} \sim$ 7770–777 km. As a result of this, it is expected that a significant portion of the beam will not undergo any scattering at all.

The RMS (root-mean-square) scattering angle θ_{rms} can be derived from the Rutherford cross section and can be estimated using [13, 14, 12]:

$$\theta_{\text{rms}} = \frac{13.6\ \text{MeV}}{\beta c p} z \sqrt{\frac{x}{X_{r,\text{vapour}}}} \left[1 + 0.038 \ln \left(\frac{x z^2}{X_{r,\text{vapour}} \beta^2} \right) \right], \tag{2}$$

where p, βc, and z are the momentum, speed, and charge number of the incident particle, and x is the thickness of the scattering medium. It is important to note that this formula holds for small scattering angles only [13]. In addition, the distribution of the scattering angles θ is Gaussian provided that particles are scattered several times [15]. θ_{rms} ranges between 0.29 - 1.10 mrad for a 18 MeV electron beam propagating in rubidium vapour of densities from $n = 1 \times 10^{14} - 10 \times 10^{14}\,\text{cm}^{-3}$, for $x = 5.5\,\text{m}$.

3. Scattering of a ∼20 MeV electron beam in rubidium vapour

To experimentally study electron beam scattering in rubidium vapour, the existing AWAKE experimental setup is used. A schematic drawing of the setup is shown in Fig. 1. The vapour source is a heated, stainless steel pipe of diameter 4 cm with two rubidium reservoirs (not shown), producing uniform vapour (<0.1 % variation) up to a density of $10 \times 10^{14}\,\text{cm}^{-3}$ [16]. The electron beam enters through an aperture. The ∼20 MeV electron beam is produced by a photoinjector [17], and transported to the entrance of the vapour source [18]. For this work, a 200 pC electron beam with normalised emittance of ∼2 mm mrad is used. The beam charge is measured using a Faraday cup, providing an absolute but invasive measurement[19]. Additionally, its relative value is continuously monitored throughout the experiment by non-invasive beam position monitors. The beam is aligned to the center of the vapour source (see Fig. 1) and focused to a vacuum spot size of $\sigma_{x,y} = (215 \pm 36, 305 \pm 35)\ \mu\text{m}$, 5.5 m downstream of the vapour source entrance (see Fig. 2a). Further details on the electron beam and the setup can be found in Ref. [20].

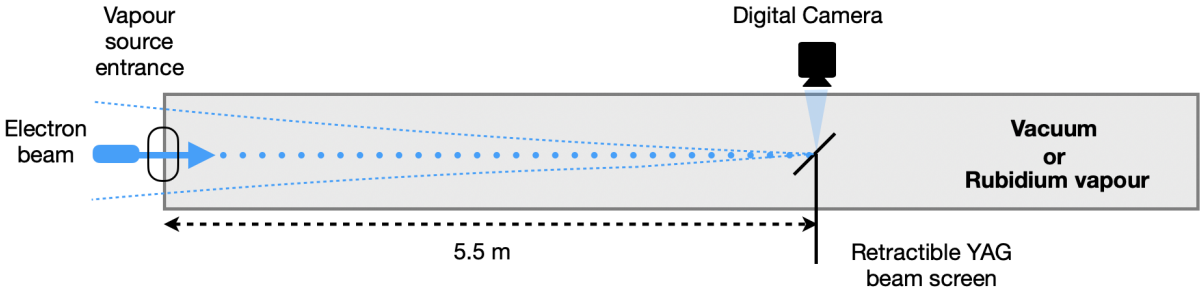

Figure 1. Schematic drawing of the experimental setup. The electron beam (blue) is focused (indicated by the dotted blue lines) onto a beam screen, located 5.5 m downstream of the vapour source entrance. Light from the beam screens is imaged through a viewport (not shown) by a digital camera (black) located outside of the vapour source. Beam propagation continues to the right in vacuum or in rubidium vapour.

The electron beam is measured by inserting a 200 µm thick scintillating YAG (Yttrium Aluminum Garnet, $Y_3Al_5O_{12}$) beam screen, that is oriented at 45 degrees to the beam propagation axis (see Fig. 1). Some of the light emitted by the YAG screen exits the vapour source through a viewport and is imaged by a digital camera located outside the vapour source. The camera image has a calibration of 23.5 µm/pixel.

3.1. Measurement results

Figure 2 shows the transverse electron beam density distribution 5.5 m downstream of the vapour source entrance, when the beam is propagating in vacuum (a) or in rubidium vapour of densities 10^{14} (b), 5×10^{14} (c), and $10 \times 10^{14}\,\mathrm{cm}^{-3}$ (d). The data shown are averages of 100 individual measurements. To avoid blurring due to beam position jitter ($\Delta_x, \Delta_y \sim 80\,\mu\mathrm{m}$), measurements are aligned to beam centroids (obtained from Gaussian fits to projections) before averaging. Gaussian fits (solid lines) to the projections of the measurements (dashed lines) indicate that beam sizes ($\sigma_{x,y}$) increase, when rubidium vapour is present.

For vapour density $10^{14}\,\mathrm{cm}^{-3}$, $\sigma_{x,y}$ increases by $\Delta\sigma_{x,y} = (37 \pm 47, 10 \pm 55)$ μm (Fig. 2b) as compared to vacuum (Fig. 2a). For vapour density $5 \times 10^{14}\,\mathrm{cm}^{-3}$, this increase is $\Delta\sigma_{x,y} = (119 \pm 46, 48 \pm 53)$ μm (Fig. 2c). Finally, for the highest measured vapour density $10 \times 10^{14}\,\mathrm{cm}^{-3}$, $\Delta\sigma_{x,y}$ increases by $(146 \pm 41,\ 78 \pm 59)$ μm compared to vacuum, (Fig. 2a). According to

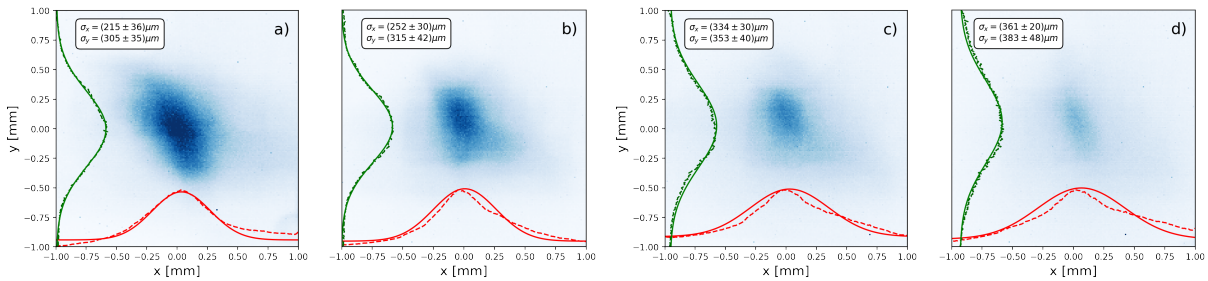

Figure 2. Electron beam distributions (average of 100 events) measured after propagation in 5.5 m of vacuum (a) and rubidium vapour with densities $10^{14}\,\mathrm{cm}^{-3}$ (b), $5 \times 10^{14}\,\mathrm{cm}^{-3}$ (c), and $10 \times 10^{14}\,\mathrm{cm}^{-3}$ (d). All plots on same colour-scale. Dashed lines show the horizontal (red) and vertical (green) projections. Solid lines show Gaussian fits to the projections. Transverse beam size $\sigma_{x,y}$, and standard deviations displayed in the plot legends.

expectations, $\sigma_{x,y}$ increases with increasing n, due to larger amount of scattering of the electrons on the rubidium atoms. The increase in $\sigma_{x,y}$ is also consistent with Eq. 2, which yields $\theta_{\mathrm{rms}} = 0.29$, 0.74 and 1.1 mrad for the densities n used in Figs. 2b-d.

Figure 3 shows the horizontal (left) and vertical (right) projections (normalised to vacuum values) from Fig. 2. The charge within the beam core decreases significantly in the presence of vapour (orange, green, and red lines) when compared to vacuum (blue line). The peak value drops from 1 (blue) to approximately 0.75, 0.6, and 0.4 for the orange, green, and red lines, respectively.

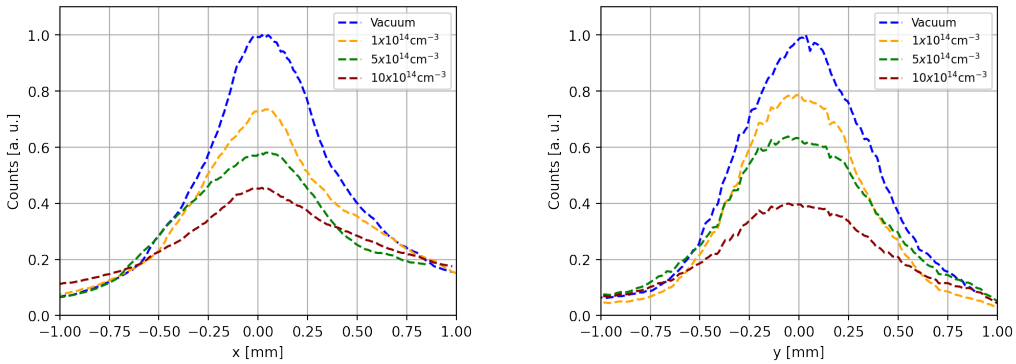

Figure 3. Horizontal (left) and vertical (right) averaged projections of 100 events and propagation in vacuum or different rubidium vapour densities, as indicated in the labels.

Since the charge in the tails of the distributions appears to increase as the core charge decreases, this observation is consistent with first principle estimates, where only a subset of the electrons scatter in vapour and form a low-density halo. These scattered electrons may fall outside the measurement range, which explains variable (to vacuum) areas under the curves. It is noted here that the electron beam charge up to the entrance of the vapour source was monitored throughout the measurements and remained constant.

3.2. GEANT4 Simulation Results

To simulate the scattering effects, the simulation code GEANT4 [23, 22, 21] was used. Similarly to the measurements, a Gaussian input beam with waist size $\sigma_{x,y} = (200, 300)$ μm, energy of 20 MeV and normalised rms emittance of $\epsilon_N = 2$ mm mrad was propagated through 5.5 m of vapour at different densities. The results are shown on Fig. 4 and are in qualitative agreement with the measurements (Fig. 3). Figure 4 confirms that electrons scatter and form a low-intensity halo around the beam core ($|x| \gtrsim 0.4$ mm, $|y| \gtrsim 0.7$ mm), especially when comparing vacuum (blue line) to a vapour density of $10 \times 10^{14}\,\mathrm{cm}^{-3}$ (red line). The simulated spot size increases due to scattering are $\Delta\sigma_{x,y} = (32, 18)$ μm for $1 \times 10^{14}\,\mathrm{cm}^{-3}$ (yellow line), $\Delta\sigma_{x,y} = (64, 43)$ μm for $5 \times 10^{14}\,\mathrm{cm}^{-3}$ (green line), and $\Delta\sigma_{x,y} = (206, 135)$ μm for $10 \times 10^{14}\,\mathrm{cm}^{-3}$ (red line). These $\Delta\sigma_{x,y}$ values are in reasonable agreement with those obtained from the measurements presented in the previous section. The comparison is limited by the accuracy of the Gaussian fits to the profiles with tails.

Comparing Figs. 3 and 4 shows that the simulated scattering effect is consistently smaller than observed in the experiment. On Fig. 4, the peak amplitude decreases from 1 to around 0.95, 0.8 and 0.65 instead of 0.75, 0.6, and 0.4 on Fig. 3 for $10^{14}\,\mathrm{cm}^{-3}$, $5 \times 10^{14}\,\mathrm{cm}^{-3}$ and $10 \times 10^{14}\,\mathrm{cm}^{-3}$, respectively. This difference may be due to simplifications in the GEANT4 simulation input parameters—for example, the neglect of electron beam dispersion or the real electron beam shape—and will be further investigated.

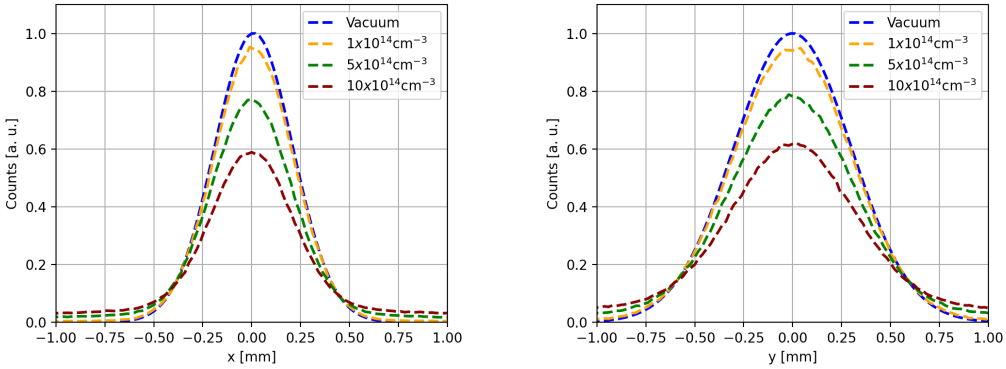

Figure 4. Horizontal (left) and vertical (right) projections of the beams after propagating in 5.5 m of vacuum, or rubidium vapour with a density indicated in the labels.

4. AWAKE Run 2c

Returning to the original question: will scattering in rubidium vapour in Run 2c significantly increase the injected electron beam size ($\sigma_{x,y} = 5$ μm at focus) or emittance ($\varepsilon_N = 2$ mm mrad)? It is estimated that the 150 MeV electron beam would propagate through at most $x = 1.65$ m of

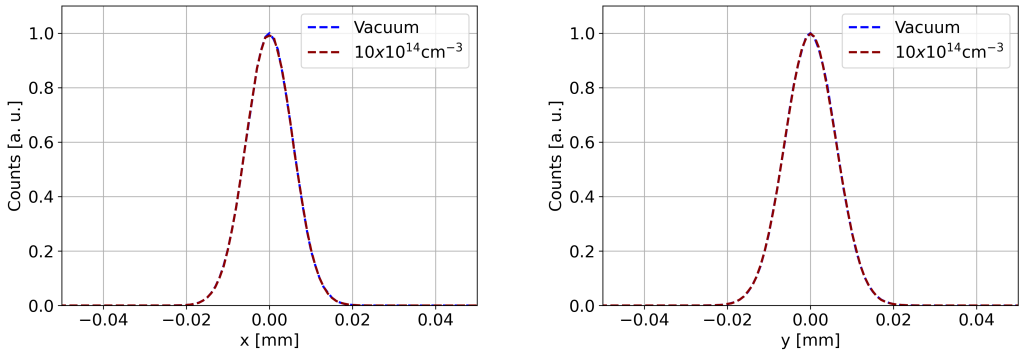

Figure 5. Horizontal (left) and vertical (right) projections of the Run 2c simulated witness beams after propagating through 1.65 m of vacuum or rubidium vapour of density 10×10^{14} cm^{-3}.

rubidium vapour at densities $1-10 \times 10^{14}$ cm^{-3}. These parameters were input to further GEANT4 simulations, shown in Fig. 5 for a density of 10×10^{14} cm^{-3}. Even at this density (which is higher than the Run 2c baseline density of 7×10^{14} cm^{-3}), Fig. 5 shows the effect on beam intensity and size to be negligible. Additionally, the transverse emittance increase $\Delta\varepsilon_N < 0.05$ mm mrad with vapour is negligible. Even if the effect of scattering is slightly underestimated in the GEANT4 simulations (as is the case for the 20 MeV beam), this result suggests that there is no problem for achieving the required AWAKE Run 2c electron beam parameters. However, further studies will be carried out to ensure that the beam parameters will meet the physics specifications.

Note that for Run 2c, scattering effects are significantly reduced compared to Run 2b due to the higher electron beam energy (150 MeV vs. ~20 MeV) and shorter vapour length (1.65 m vs. 5.5 m). In this case the GEANT4 simulations no longer assume a Gaussian model but instead switch to a Molière model (based on a Landau distribution), which can also take large scattering angles into account [25]. As a result, Eq. 2 can no longer be used to calculate θ_{rms}.

5. Conclusions

The scattering effect of a 5.5 m long rubidium vapour column on a ~20 MeV electron beam is studied for densities relevant to the AWAKE experiment ($1-10 \times 10^{14}$ cm^{-3}). The effect is

estimated using Rutherford scattering, measured experimentally, and simulated with GEANT4. While the beam size increase shows generally good agreement across methods, the GEANT4 simulations consistently predict a smaller decrease in beam density due to scattering than is observed in the measurements. Future work will use more realistic electron beam parameters in the simulation input and aim for round and Gaussian-shaped beams in the measurements.

Finally, GEANT4 simulations are used to examine the scattering effects for AWAKE Run 2c, involving a 150 MeV electron beam passing through a 1.65 m long rubidium vapour column at a density of $10 \times 10^{14}\,\mathrm{cm}^{-3}$. The impact on beam intensity, size, and emittance is found to be negligible.

References

[1] AWAKE Collaboration, "Acceleration of electrons in the plasma wakefield of a proton bunch", *Nature*, vol. 561, pp. 363-7, 2018. doi:10.1038/s41586-018-0485-4

[2] E. Gschwendtner *et al.* (AWAKE Collaboration), "The AWAKE run 2 programme and beyond", *Symmetry* vol. 14, p. 1680, 2022. doi:10.3390/sym14081680

[3] N. Z. van Gils, M. Turner, G. Z. Della Porta, F. Pannell, V. Bencini, A. Gerbershagen and E. Gschwendtner, submitted to *Proc. 6th European Advanced Accelerator Concepts Workshop (EAAC'23)*, 2023.

[4] D. Cooke *et al.* (AWAKE Collaboration), "Measurement of the emittance of accelerated electron bunches at the AWAKE experiment", arXiv preprint arXiv:2411.08681, 2024.

[5] M. Turner *et al.* "External Electron Injection for the AWAKE Experiment", in *Proc. 18th Adv. Acc. Concepts Workshop (AAC'18)*, Colorado, USA, 2018. doi:10.1109/AAC.2018.8659402

[6] V. K. Berglyd Olsen, E. Adli and P. Muggli, "Emittance preservation of an electron beam in a loaded quasilinear plasma wakefield", *Phys. Rev. Accel. Beams*, vol. 21, p. 011301, 2018. doi:10.1103/PhysRevAccelBeams.21.011301

[7] R. Ramijawan *et al.*, "Design of the proton and electron transfer lines for AWAKE Run 2c", in *Proc. 12th Int. Particle Accelerator Conf. (IPAC'21)*, Campinas, SP, Brazil. doi:10.18429/JACoW-IPAC2021-MOPAB241

[8] M. Turner *et al.* (AWAKE Collaboration), "Experimental Observation of Plasma Wakefield Growth Driven by the Seeded Self-Modulation of a Proton Bunch", *Phys. Rev. Lett.*, vol. 122, p. 054801, 2019. https://journals.aps.org/prl/abstract/10.1103/PhysRevLett.122.054801

[9] E. Adli *et al.* (AWAKE Collaboration), "Experimental Observation of Proton Bunch Modulation in a Plasma at Varying Plasma Densities", *Phys. Rev. Lett.*, vol. 122, p. 054802, 2019. https://journals.aps.org/prl/abstract/10.1103/PhysRevLett.122.054802

[10] F. Batsch *et al.* (AWAKE Collaboration), "Transition between Instability and Seeded Self-Modulation of a Relativistic Particle Bunch in Plasma", *Phys. Rev. Lett.*, vol. 126, p. 164802, 2021. https://journals.aps.org/prl/abstract/10.1103/PhysRevLett.126.164802

[11] Y. Tsai, Pair production and bremsstrahlung of charged leptons. *Rev. Mod. Phys.*. **46**, 815-851 (1974,10), https://link.aps.org/doi/10.1103/RevModPhys.46.815

[12] S. Navas *et al.* [Particle Data Group], *Phys. Rev. D* **110** (2024) no.3, 030001 doi:10.1103/PhysRevD.110.030001

[13] H. A. Bethe, "Molière's theory of multiple scattering", *Phys. Rev.* **89**, 1256–1266, (1953). doi:10.1103/PhysRev.89.1256

[14] G. R. Lynch and O. I. Dahl, "Approximations to multiple Coulomb scattering," *Nucl. Instrum. Methods Phys. Res., Sect. B*, vol. 58, no. 1, pp. 6–10, May 1991. doi:10.1016/0168-583x(91)95671-y

[15] E. Fischer, "Residual gas scattering: beam intensity and interaction rate in proton storage rings", CERN, 1967. https://cds.cern.ch/record/296970

[16] P. Muggli, M. Bergamaschi, J. Pucek, D. Easton, J. Pisani, and J. Uncles, "Plasma light as diagnostic

for wakefields driven by developing self-modulation of a long particle bunch", in *Proc. 20th Adv. Acc. Concepts Workshop (AAC'22)*, Long Island, NY, USA, 2022.

[17] Y. Kim *et al.*, "Commissioning of the electron injector for the AWAKE experiment", *Nucl. Instrum. Meth. in Phy. Res.* A, vol. 953, p.163194, 2020. doi:10.1016/j.nima.2019.163194

[18] J.S. Schmidt *et al.*, "Status of the proton and electron transfer lines for the AWAKE Experiment at CERN", *Nucl. Instrum. Meth. in Phy. Res.* A, vol. 829, pp 58-62, 2016. doi:10.1016/j.nima.2016.01.026

[19] N. Z. van Gils *et al.*, "Preparation for Realisation of External Electron Injection for AWAKE Run 2b", in *Proc. 15th Int. Particle Accelerator Conf. (IPAC'24)*, Nashville, TN, USA, May 2024, paper MOPR42, pp. 3709-12. doi:10.18429/JACoW-IPAC2024-MOPR42

[20] N. Z. van Gils *et al.*, "Verification of electron beam alignment and optics for external off-axis injection in AWAKE Run 2b", *Nucl. Instrum. Meth. in Phy. Res.* A, vol. 1072, 170204, 2025. doi:10.1016/j.nima.2025.170204

[21] S. Agostinelli *et al.*, "Geant4—a simulation toolkit", *Nucl. Instrum. Meth. in Phy. Res.* A, vol. 506, pp. 250-303, 2003. https://www.sciencedirect.com/science/article/pii/S0168900203013688

[22] J. Allison *et al.*, "Geant4 developments and applications" *IEEE Transactions On Nuclear Science*, vol. 53, pp. 270-278, 2006. doi:10.1109/TNS.2006.869826

[23] J. Allison *et al.*, "Recent developments in Geant4", *Nucl. Instrum. Meth. in Phy. Res.* A, vol. 835, pp. 186-225 , 2016. https://www.sciencedirect.com/science/article/pii/S0168900216306957

[24] A. Latina, "The Tracking Code RF-Track and Its Application," JACoW **HB2023**, 245-248, 2024. https://doi.org/10.18429/JACoW-IPAC2021-THPAB203

[25] Geant4, "Physics reference manual", Version: geant4 9.0, 2020. https://geant4-userdoc.web.cern.ch/UsersGuides/IntroductionToGeant4/html/index.html